JPET Fast Forward. Published on April 11, 2006 as DOI: 10.1124/jpet.106.101915

INTERACTION OF FUNCTIONALIZED SUPERPARAMAGNETIC IRON OXIDE NANOPARTICLES WITH BRAIN STRUCTURES.

Feride CENGELLI, Dusica MAYSINGER, Florianne TSCHUDDI-MONNET, Xavier MONTET, Claire COROT, Alke PETRI-FINK, Heinrich HOFMANN, and Lucienne JUILLERAT-JEANNERET

University Institute of Pathology (F.C., L.J.-J.), CHUV, Lausanne, Switzerland; Department of Pharmacology (D.M.), McGill University, Montréal, Canada; Institute of Physiology (F.T.-M.), University of Lausanne, Switzerland; Department of Cell Physiology and Metabolism and Medical Radioloy (X.M.), University of Geneva, Switzerland; Guerbet (C.C.), Research, Roissy, France; and Institute of Materials Science (A.P.-F., H.H.), Laboratory of Powder Technology, Swiss Federal Institutes of Technology (EPFL), Lausanne, Switzerland.

Running title : Magnetic nanoparticles interaction with brain structures

Corresponding author :

Dr Lucienne Juillerat, PhD, PD, MER

University Institute of Pathology; Bugnon 25; CH-1011 Lausanne, Switzerland

phone : +41 21 314 7173, fax : +41 21 314 7115, e-mail : lucienne.juillerat@chuv. ch

Number of text pages: 35

Number of tables: 4

Number of figures: 7

Number of references: 40

Number of words in Abstract: 245

Number of words in Introduction: 502

Number of words in Discussion: 1347

List of abbreviations: BBB: blood-brain barrier; DAF: 5-dodecanoyl-aminofluorescein; DAPI: 4',6-diamidine-2'-phenylindole; FCS: fetal calf serum; MRI: magnetic resonance imaging; LPS: lipopolysaccharide; MTT: 3-(4,5-dimethylthiazolyl)-2,5-diphenyl-2H-tetrazolium bromide; PBS: phosphate-buffered saline; PVA: polyvinyl alcohol; SPIONs: superparamagnetic iron oxide nanoparticles

Section: Neuropharmacology

Abstract

Super Paramagnetic Iron Oxide Nanoparticles (SPIONs) combined with MRI are under clinical evaluation to enhance detection of neurodegenerative diseases. A major improvement would be to link therapeutic drugs to the SPIONs to achieve targeted drug delivery, either at the cell surface or intracellularly, together with active disease detection, without inducing cell reaction. Our objectives were to define the characteristics of SPIONS able to achieve cell-specific interaction with brain-derived structures. Our system consisted in an ironoxide core (9-10 nm diameter) coated either with dextran (Sinerem and Enorem) or various functionalized polyvinylalcohols (PVA) (PVA-SPIONs). We investigated the cellular uptake, cytotoxicity and interaction of these various nanoparticles with brain-derived endothelial cells, microglial cells and differentiating 3-dimensional aggregates. None of the nanoparticles coated with dextran or the various PVAs was cytotoxic or induced the production of the inflammatory mediator NO used as a reporter for cell activation. AminoPVA-SPIONs were taken up by isolated brain-derived endothelial and microglial cells at a much higher level than the other SPIONs, and no inflammatory activation of these cells was observed. AminoPVA-SPIONs did not invade brain cells aggregates lower than the first cell layer and did not induce inflammatory reaction in the aggregates. Fluorescent aminoPVA-SPIONs derivatized with a fluorescent reporter molecule and confocal microscopy demonstrated intracellular uptake by microglial cells. Fluorescent aminoPVA-SPIONs were well tolerated by mice. Therefore functionalized aminoPVA-SPIONs represent biocompatible potential vector systems for drug delivery to the brain which may be combined with MRI detection of active lesions in neurodegenerative diseases.

Introduction

Nanotechnologies and nanostructures are becoming an option in human medical application, including imaging or the delivery of therapeutic drugs to cells, tissues and organs. Most of these latter applications would require that drug-loaded nanoparticles enter organ and tissues, and are taken up by cells. Several studies have shown that the tissue, cell and even cell organelles distribution (Alexiou et al., 2000; Savic et al., 2003) of drugs may be controlled and improved by their entrapment in colloidal nanomaterials, mainly of the micellar structure, such as nanocontainers. The development of a large variety of colloidal dispersions of Super Paramagnetic Iron Oxide Nanoparticles (SPIONs) has added a supplementary function to nanomaterials, their magnetic properties, which can lead to a range of new biological, biomedical and diagnostic applications. In particular, the application of the different forms of iron oxides for radiological diagnostic procedures, to document vascular leakage, macrophage imaging or cell tracking (Weissleder et al., 1997; Ruehm et al., 2001; Brigger et al., 2002; Hoehm et al., 2002; Kircher et al., 2003; Corot et al., 2004; Neuwelt et al., 2004; Raynal et al., 2004; Sundstrom et al., 2004; Triverdi et al., 2004; Dalrup et al., 2005) is gaining wide acceptance in radiological practice, but these agents are only very poorly taken up by cells, depending on their size or the expression of the scavenger receptors by cells (Ruehm et al., 2001; Corot et al., 2004; Raynal et al., 2004; Triverdi et al., 2004).

Therefore the next challenge will be to develop and define the chemical and biophysical characteristics of biocompatible SPIONs which are able to intracellularly deliver therapeutic drugs, in particular in neurodegenerative diseases without inducing deleterious cell reaction, coupled to the detection of active lesions. SPIONs are able, under some conditions, to pass the blood-brain barrier, either by direct transport (Lockman et al., 2003; 2004; Kreuter, 2004; Muller and Keck, 2004), or using an indirect route via the olfactory bulb (Obersdörster et al, 2004; Kandimalla and Donovan, 2005) and to document active lesions by MRI in

neurodegenerative disorders (Corot et al., 2004). However, particles that can penetrate into the brain, and other organs, also pose a potential health risk (Obersdörster, 2004; Colvin, 2003; Borm and Kreyling, 2004; Hoet et al., 2004). A better understanding of how properties of nanoparticles define their interactions with cells, tissues and organs in humans and animals is a considerable scientific challenge but one that must be addressed to ascertain the feasibility of using nanobiotechnologies in biomedical applications..

In a preliminary approach, we have prepared and characterized various polyvinyl-alcohol-coated SPIONs (Chastellain et al., 2004; Petri-Fink et al., 2005) which displayed the potential to interact with non-phagocytic human tumor cells. In order to evaluate their brain biocompatibility and their potential for drug delivery to the brain, we determined the uptake of and inflammatory reaction towards SPIONs of various size and coating characteristics, using either isolated brain cells, *i.e.* the brain macrophages (microglial cells) and endothelial cells forming the blood-brain barrier, and differentiating aggregated three-dimensional brain cells at different stages of differentiation.

Methods

SPIONs

Iron oxide nanoparticles (ferrofluid) were prepared according to described methods (Massart et al., 1995; van Ewijk et al., 1999; Chastellain et al., 2004). Briefly, SPIONs were prepared by alkaline co-precipitation of ferric (0.086 M) and ferrous (0.043 M) chlorides (Fluka, Buchs, Switzerland). After washing with water, the black precipitate was refluxed in 0.8 M nitric oxide-0.21 M $Fe(NO_3)_3.9H_2O$ (Fluka) for 1 h, cooled and the brown precipitate was dispersed in H_2O, then dialyzed for 2 days against 0.01 M nitric acid. The dialyzed iron oxide nanoparticles were mixed with the various polyvinyl alcohol (PVA) polymers as previously described (Chastellain et al., 2004; Petri-Fink et al., 2005) and the pH was adjusted to 7 to obtain PVA-coated nanoparticles, either native-, amino-, carboxylate- and thiol-PVA-SPIONs. For the experiments described here the ratio of polymer/iron was 10 (45 mg polymer/ml and 4.5 mg iron/ml, final concentrations), and the ratio of PVA/functionalizedPVA copolymer was 45 (mass ratio). Dextran-coated Endorem (Endorem®, Guerbet, G 534-14, lot 134, 11.2 mg Fe/ml) and Sinerem (Ferrumoxtran-10, AMI227, Guerbet, G534-25, lot ADS03, 20 mg Fe/ml) were provided by Guerbet, France. The various nanoparticles used in this study and their biochemical characteristics are summarized in **Table 1 and Figure 1**. Cy3.5-SPIONs or Cy5.5-SPIONs were prepared by reacting under shaking 500 µl amino-PVA-SPIONs ($2\text{-}5x10^{15}$ nanoparticles/ml, 4.5 mg iron/ml) with 500 µl Cy3.5-N-hydroxy-succinimide ester or Cy5.5-N-hydroxy-succinimide ester (30 mmole NH_2-labelling capacity, Cy3.5- or Cy5.5-monoreactive dye, Amersham Biosciences, Upsala, Sweden) in 25 mM sodium carbonate buffer pH 9.5 for 2 h in the dark at room temperature, followed by sequential gel filtration through pre-packed Sephadex G-25 columns (8.3 ml bed volume) (Amersham Biosciences) first in 25 mM sodium phosphate buffer pH 7.5, then in nanopure water.

Cells and cell culture treatments with the various nanoparticles.

The characteristics and culture conditions of the rat brain-derived endothelial EC219 (Juillerat-Jeanneret et al., 1992; 2003) and the murine N9 et N11 microglial (Murata et al., 1994; 1997) (kindly provided by P Ricciardi-Castagoli, Milan, Italy) cell lines have been described. EC219, N9 and N11 cells were previously shown to produce nitric oxide under inflammatory stress (Murata et al., 1994; 1997). Cells were routinely maintained in their culture medium containing FCS and antibiotics (both from Gibco, Invitrogen, Basel, Switzerland). Three days prior to experiments, the cells were detached in trypsin-EDTA (Gibco) and grown in complete medium in 96- or 48-well plates (Costar, Corning, NY, USA). On the day of experiment, medium was changed to fresh complete medium, and the various nanoparticles preparations (cf above) were added for the concentration, time and temperature indicated, together with 1 µg/ml lippopolysaccharide (LPS, Sigma, Buchs, Switzerland) when indicated. At the end of the experiment, either the MTT (3-(4,5-dimethylthiazolyl)-2,5-diphenyl-2H-tetrazolium bromide, Sigma) test was performed for the two last hours to determine cell viability (cf below) or the cell layers were washed twice in saline, or when indicated for 5 min at room temperature in 0.15 M Na-acetate buffer pH 5.2 to remove cell surface nanoparticles, and cellular iron content was quantified (cf below). Alternatively, histological staining of iron or confocal microscopy was performed (cf below).

Aggregate cultures and treatments

Brain-cell derived aggregates were prepared from the telencephalon of E16 rat embryos (OFA/SPF, BRL, Füllinsdorf, Switzerland) and maintained in defined medium under continuous giratory agitation, essentially as previously described (Honegger and Tschuddi-Monnet, 2000). On days 7, 14, 21 or 28, aminoPVA-SPIONs (2.5 µl nanoparticles/ml culture

medium, 11.3 μg iron/ml) were added to the aggregates for 48 h and then 5 ml out of 8 ml per flask of culture medium was changed to fresh medium containing aminoPVA-SPIONs at the same concentration for another 24 h. Then out of 8 ml 5 ml per flask were replaced by fresh culture medium without SPIONs, and the culture was continued for 48 h. Aggregates were harvested by sedimentation, the culture supernatants were frozen (for further determinations of NO) and the aggregates were washed in PBS, embedded (Tissue-Tek™, Sakura, Zoeterwoude, NL) and frozen in isopentane cooled in liquid nitrogen for histochemistry. This model has been previously shown to be relevant in the evaluation of brain inflammation (Juillerat-Jeanneret et al., 2003).

Evaluation of cell viability, protein content and NO

The evaluation of MTT reduction to quantify metabolically active cells was performed essentially as previously described (Petri-Fink et al., 2005). Cell layers were extracted in PBS-0.1% Triton X-100 and protein content was quantified with the BCA kit (BCA™, Pierce, Socochim, Lausanne, Switzerland) and bovine serum albumin as standard. The production of NO was measured in culture supernatants as the stable NO-derivative NO_2^- with the Griess reagent, essentially as previously described (Murata et al., 1994).

Total cell iron determination

The cell layer was dissolved for 1 h in 6N HCl (125 μl/well of a 48-well plate), then 125 μl of a 5% solution of $K_4[Fe(CN)_6]\cdot 3H_2O$ (Merck, Dietikon, Switzerland) in H_2O was added for 10 min and the absorbance was read at 690 nm in a multiwell plate reader (iEMS, Labsystems, BioConcepts, Allschwil, Switzerland). A standard curve of an aqueous $FeCl_3\cdot 6H_2O$ (Merck) solution was treated in the same conditions to quantify the amount of cell-bound iron.

JPET Fast Forward. Published on April 11, 2006 as DOI: 10.1124/jpet.106.101915
This article has not been copyedited and formatted. The final version may differ from this version.

Histochemical determination of iron

Histological sections (5 μm) of frozen aggregates were cut or cells were grown on histological glass slides in medium containing 10% FCS and antibiotics. Then medium was changed to fresh complete medium containing 1μl aminoPVA-SPION (4.5 μg iron/ml culture medium) for 5 to 240 min at 37°C, the medium was aspirated, the cell layer was washed 3 times, fixed for 15 min in 4% buffered paraformaldehyde at room temperature, washed, and air-dried. The cell layer was exposed for 15-30 min at room temperature to a 1:1 solution of 1N HCl and 10% K_4 $[Fe(CN)_6]$ (Fluka, Buchs, Switzerland) in H_2O, washed in distilled water, counterstained with Nuclear Fast Red, dehydrated in graded alcohol and mounted. Slides were photographed under a Nikon digital camera.

Lectin histochemistry

Histological sections (5 μm) of aggregates were post-fixed for 15 min in 4% buffered paraformaldehyde and incubated overnight at 4°C in a solution of horseradish peroxidase-conjugated *Bandeirea simplicifolia*-1 lectin (Sigma, 12.5 μg/ml in 0.1 M Tris-NaCl - 1% Triton X-100 pH 7.4), then exposed to 0.002 % diaminobenzamidine (Fluka) and counterstained with hematoxylin (Honegger and Tschuddi-Monnet, 2000; Juillerat-Jeanneret et al., 2003).

Confocal microscopy

N9 murine microglial cells were grown in Iscove's Modified Dulbecco's Medium (Sigma) containing 5% FCS and free of phenol red. Two hours prior to treatments, cells were washed and media was replaced with FCS-free media. Cells were seeded into 8-well chambers (Lab-Tek®, Nalge Nunc International, Rochester, NY, USA) at a density of 10^5 cells/cm^2. Cy3.5-aminoPVA-SPIONs were added (20 μg iron/ml, final concentration), and cells incubated for

different time periods from 1 min to 20 h. Plasma membranes were labeled with 5-dodecanoyl-aminofluorescein (DAF, 1 μM, Molecular Probes, Eugene, OR, USA) and nuclei using 4',6-diamidine-2'-phenylindole (DAPI) staining (10 μM, 10 min, Sigma). Cells were washed once either with PBS or acidified wash (0.5 M NaCl, 0.2 M CH_3COOH, pH 2.5), once with PBS and then once with FCS-free medium to remove any non-specifically adsorbed SPIONs or free fluorescent dye. No background cell fluorescence was detected under the settings used. Microscopy was performed using a confocal Laser Scanning LSM 510 Zeiss microscope equipped with the following lasers: (i) HeNe LASOS LGK 7786 P/Power supply 7460 A 543 nm 1mW, (ii) Argon LASOS LGK 7812 ML-1/LGN: 458, 488, 514 nm 25 mW, Laser class 3D, and (iii) Titanium-Sapphire The Coherent Mira Model 900-f Laser tunable from 710 to 1000 nm for two photon microscopy (set to pulse at 800 nm). Excitation/emission maxima for the dyes are: DAF 495/518 nm; DAPI 358/461 nm; Cy3.5 581/596 nm.

Animal evaluations

C57BL6 mice (6-8 weeks old, Charles River/Iffa Credo, Lyon, France) were injected on day 0 with Cy5.5-aminoPVA-SPIONs (3 mg iron/kg body weight, adjusted to 100 μl/mouse with sterile PBS, stock solution of Cy5.5-aminoPVA-SPIONs: 4.5 mg iron/ml) and examined 24 h later, then killed and the brains were either frozen or fixed for 48 h in buffered formaldehyde and embedded in paraffin. Histological sections (5 μm) were cut and Prussian Blue histological determination of iron was performed as described above. Frozen samples were cut at 8 μm mounted in Fluoromount-G (Fluoromount-G®, SouthernBiotech, Birmingham, AL) and examined under a fluorescence microscope. This protocol has been approved by the Ethics Committee for Animal Experimentation of the Canton of Geneva.

Calculations of results

Each experiment was repeated in triplicate wells at least two times. Means and standard deviation were calculated.

For confocal microscopy, data were analyzed using SYSTAT 10 (SPSS, Chicago, IL, USA). Statistical significance was determined by analysis of variance (ANOVA) followed by post-hoc Tukey's test. Differences were considered significant where $p<0.05$.

Results

First we determined the uptake (**Table 2**) of ultra-small dextran-coated SPIONs (Sinerem, hydrodynamic diameter 15-30 nm) by brain-derived rat EC219 endothelial cells and murine N9 and N11 microglial cells exposed to various concentration of Sinerem. Endothelial EC219 cells, even when exposed to high concentrations of Sinerem and for long exposure time did not take up Sinerem, whereas only N11 cells took up Sinerem at very low levels. In co-cultures of EC219 cells with N9 or N11 cells (**Table 3)**, either resting cells or LPS-activated cells, no increase in cell-bound iron was observed (**Table 3**). In untreated cells, the apparent iron content as determined by the Prussian Blue reaction in the absence of added nanoparticles were 30 (EC219 cells), 35 (N9 cells) and 45 (N11 cells) μM.

In order to further determine the effects of the SPION particle size and of inflammatory cell activation for efficient cell uptake, we evaluated whether dextran-coated SPIONs with a larger hydrodynamic size (beads) (Endorem, hydrodynamic diameter 80-150 nm) would display an increased uptake by EC219 and N11 cells, either resting or LPS-activated cells (**Table 4**). In EC219 endothelial cells, Endorem uptake was low, and did not increase with time of exposure or the presence of LPS (**Table 4**), however, endothelial cells did respond to LPS by increasing NO release (results not shown). We have previously shown that EC219, N9 and N11 cells respond to inflammatory stimuli, including LPS, by producing NO (Murata et al., 1994; 1997). In N11 microglial cells, spontaneous uptake was slow, but increased with time (**Table 4**), the amount of Endorem added to the cells (**Figure 2**). LPS addition to N11 cells increased SPION uptake (**Table 4**) and NO release (results not shown). However, LPS addition must be performed simultaneously and not 24 h prior to Endorem addition in order to observe such an effect. However, whatever the culture conditions, only a low percentage (less than 1%) of Endorem added to microglial cells was taken up by these cells.

Therefore, the uptake of dextran-coated SPIONs by brain-derived cells was slow and low, whatever the hydrodynamic size of the SPIONs and the cell activation state. These characteristics make these particles well suited for magnetic imaging, but not for tissue and intracellular drug delivery. Thus we evaluated whether modification of the polymer coating of SPIONs would improve their interaction with brain-derived cells, as previously shown for human melanoma cells (Petri-Fink et al., 2005).

NativePVA-, carboxylatePVA- or thiolPVA-SPIONs were not taken up by N11 microglial cells, and only aminoPVA-SPIONs were taken up by N11 cells (**Figure 3A**). EC219 cells also took up aminoPVA-SPIONs (**Figure 3B**). However, uptake saturation was reached at lower aminoPVA-SPION concentration in brain-derived EC219 endothelial cells than N11 microglial cells. To determine whether the uptake of aminoPVA-SPIONs induced inflammatory activation of cells, we measured NO in the culture supernatants of cells exposed for up to 24 h to aminoPVA-SPIONs. NO production was never detected (results not shown). In order to evaluate whether all cells, or only some cells of a culture were able to take up the aminoPVA-SPIONs, we exposed N11 and EC219 cells grown on histological slides to aminoPVA-SPIONs for increasing time periods, and performed iron histological staining (**Figure 4**). These experiments demonstrated a time-dependent cell-associated increase of iron in all cells, comparable to total iron determination in cell extracts (**Figure 3**) and the pattern of iron location suggested internalization by the cells.

In order to confirm internalization of amino-SPIONs by cells, we prepared aminoPVA-SPIONs of which one out of ten amino-group was covalently derivatized by the fluorescent reporter molecule Cy3.5 (**Figure 5A**). Iron uptake by N9 cells was time- and temperature-dependent (**Figure 5B**) and cell-bound fluorescence demonstrated the same pattern than iron uptake (**Figure 5C**), however with faster time-course efficacy. Identical information was obtained with N11 cells (**Figure 6C**). In order to determine whether the reporter fluorophore

was effectively intracellular, we performed confocal microscopy. In N9 cells (nucleus = blue (DAPI), membrane = green (DAF), Cy.3.5 = red) exposed for short exposure (20 min) to Cy3.5-aminoPVA-SPIONs, no uptake was observed (**Figure 6A**), whereas after 20 h, intracellular location of the fluorophore was documented (**Figure 6B**). This time-course paralleled the uptake of iron by N9 cells as determined by iron histological staining (**Figure 6C**). From the aspect of cells under phase contrast and confocal microscopy, the absence of cytotoxicity was evident.

Therefore these experiments demonstrated that brain-derived endothelial and microglial cells internalize aminoPVA-SPIONs, and that uptake did not result in the production of NO as a marker of inflammatory activation of these cells. In order to determine whether these aminoPVA-SPIONs have the potential to be taken up by and massively invade brain parenchyma and whether they would induce brain activation, we used a 3-dimensional brain-cell aggregate culture model, at various stages of neural cell differentiation (Honegger and Tschuddi-Monnet, 2000). In this model, dissociated embryonic neural cells are reassociated under gyratory culture conditions, and astrocytes, neuron, oligodendrocytes, and microglial cells differentiate with the time in culture (Honegger and Tschuddi-Monnet, 2000). After 1 week (undifferentited aggregates) to 4 weeks (differentiated aggregates) in culture, aggregates were exposed to aminoPVA-SPIONs and histological iron determination and BS-1 lectin staining (an histological marker of microglial activation) as well as determination of NO in the aggregate culture medium were performed. Different patterns of iron staining were observed with the stages of differentiation, however at any stage only the tanicytes (the specific astrocytic cell external layer of brain ventricles) of aggregates demonstrated detectable iron uptake (**Figure 7A**), and no deep brain aggregate penetration was observed. At early differentiation stages (1-2 weeks), iron staining was more irregular and sometimes located in cells of the second layer of the aggregates, whereas at higher differentiation stages

(3-4 weeks), when the aggregates structures are well organized, iron staning was observed only in cells of the external layer. No increase in BS-1 lectin staining was observed at any stage of differentaition (**Figure 7B**, 2 weeks, other stages not shown) and NO was not detected in the aggregate culture medium (results not shown), confirming the absence of inflammatory activation and the biocompatibility of these nanoparticles for brain tissue.

In order to evaluate biocompatibility *in vivo*, we injected normal mice with aminoPVA-SPIONs at a concentration comparable to the iron dosages used in patients for MRI-enhanced evaluation of liver disorders. Following i.v. injection of Cy5.5aminoPVA-SPIONS into mice no massive blood clotting, or renal, hepatic, cardiovascular, respiratory side-effects for at least 24 h was observed demonstrating *in vivo* biocompatibility. Histological determination of iron demonstrated SPIONs capture in spleen>liver>brain = kidney. In the brain, only scattered SPIONs particles could be detected (results not shown).

Discussion

Treatment options for a number of human disorders, in particular those of the brain, are often limited by the high drug concentrations required for efficacy, the presence of drug resistance mechanisms, and the poor cell selectivity of therapeutic agents. These characteristics are especially important in the context of neurodegenerative disorders. The brain is separated from the bloodstream by the blood-brain barrier (BBB) (Risau and Wolburg, 1990), a highly specialized vascular system consisting of endothelial cells, pericytes and astrocytes. The presence of tight junctions between cells of the BBB protects the brain from blood-borne pathogens and chemicals, but also impedes the access of therapeutic drugs. In certain disorders, however, such as neurodegeneration and brain cancer, the BBB becomes compromised which creates a window for drug delivery (Muldoon et al., 1999; Lockman et al., 2004). Alternatively, therapeutics agents can be transported across an intact BBB by hijacking the endogenous transport systems of the cerebral vasculature (Lockman et al., 2003). Another approach to drug delivery to the brain is to utilize the connection that exists between the nervous and olfactory systems (Borm and Kreyling, 2004). Regardless of the route used to deliver drugs into the brain, the diffusion of the drug delivery devices into the brain parenchyma must be controllable and must avoid activation of microglial cells, since the brain possesses its own macrophage population, the microglia, which are involved in the development of neurodegenerative disorders (Perry et al., 1993) and could be activated by the treatments. Macrophages in inflammatory areas, from the brain or other tissues, are main targets for nanoparticles, whether magnetic or not (Ruehm et al., 2001; Corot et al., 2004; Raynal et al., 2004; Triverdi et al., 2004; Chellat et al., 2005). In the present manuscript, our experimental approaches were designed to evaluate whether i) intracellular uptake by brain cells of functionalized SPIONs is possible and would be harmful and inflammation-inducing

for brain-derived cells and structures, and whether ii) massive invasion of the brain would be observed, which is not a desirable effect.

Therefore, our goals in the present study were to define the biophysical, biological and biochemical characteristics of SPIONs with such properties. Using the rat brain-derived EC219 endothelial cells, the murine N9 and N11 microglial cells, and differentiating aggregate brain cells in three-dimensional cultures, we have evaluated the cellular uptake, the cytotoxicity, and the interaction of these cells with various nanoparticles. Macrophages and endothelial cells express organ-specific properties, but macrophages and endothelial cells of rodent origin (Murata et al., 1994; 1997), as well as rodent brain-cells in aggregate culture (Juillerat-Jeanneret et al., 2003) have been shown to produce nitric oxide following stimulation, which represents a convenient way to evaluate their activation following exposure to SPIONs. SPIONs coated with dextran polymer, either ultra-small, $\leq$ 30 nm, or beads of 80-150 nm were well tolerated by endothelial and microglial cells, but their cellular uptake was low. Ultrasmall, $\leq$ 40 nm, SPIONs coated with either polyvinylalcohol (PVA) or with PVA which has been derivatized on the hydroxyl groups with either carboxylate or thiol groups were well tolerated by cells, but no cell uptake was observed. AminoPVA-SPIONs were internalized, core iron oxide and polymer, by cerebral cells, either isolated cells in two-dimensional culture, or differentiated cells in three-dimensional aggregate cultures. Cationic molecules display increased cell uptake, but may also display increased cytotoxicity. Importantly, no cellular reaction was observed following cellular uptake of aminoPVA-SPIONs, as estimated by nitric oxide production or the evaluation of microglial activation. These nanoparticles were also well tolerated when injected into normal mice.

Previous experiments using magnetic approach to drug targeting have been performed by some groups with magnetic particles or magnetic liposomes ranging from 10 μm to 100 nm, loaded with chemotherapeutic agents (Alexiou et al., 2000; Rudge et al., 2001). Some positive

effects were obtained, in particular a decrease of general toxicity of the agents, due to generally lower doses required. Magnetically-controlled drug targeting and delivery requires magnetic nanoparticles with high magnetization properties and the possibility of surface derivatization for drug attachment in order to achieve magnetic drug delivery. SPIONs, or super paramagnetic nanoparticles with an ironoxide core diameter of less than 10 nm, exhibit outstanding magnetic properties, as they show no magnetization in the absence of a magnetic field but become strongly magnetized in the presence of one. Biocompatible superparamagnetic nanoparticles have been developed for in vivo biomedical applications mainly in magnetic resonance imaging (Weissleder et al., 1997), and have only been evaluated pre-clinically in tissue-specific delivery of therapeutic agents (Lubbe et al., 1996). Two advantages of SPIONs are their low toxicity to humans and the possibility to exploit their superparamagnetic properties (Weissleder et al., 1997; Ruehm et al., 2001; Brigger et al., 2002; Hoehm et al., 2002; Kircher et al., 2003; Corot et al., 2004; Neuwelt et al., 2004; Raynal et al., 2004; Sundstrom et al., 2004; Triverdi et al., 2004; Dalrup et al., 2005). Although the use of SPIONs as magnetic resonance imaging contrast agents is established, their potential as drug targeting and drug delivery agents is still in early stage of evaluation.

In drug delivery application, the critical step is the transport across cell layers (Koch et al., 2005) and the internalization of nanoparticles into specific cells, a process often limited by poor targeting specificity and low internalization efficiency of therapeutic ligands grafted on the nanoparticles. A number of studies have addressed the cell-surface binding or cell uptake of functionalized SPIONs. Surface modification of the polyethyleneglycol film of SPIONs with folic acid was shown to decrease their uptake by mouse macrophages and increase their uptake by human cancer cells (Zhang et al., 2002), and albumin coating of anionic SPIONs led to internalization by cells (Wilhelm et al., 2003). Dextran-coated SPIONs of 150 nm, but not of 10 nm, were shown to be taken up by macrophages in a process involving type I and II

scavenger receptor-mediated endocytosis (Raynal et al., 2004). Macaque T cells labelled with monocrystalline SPIONs following adsorptive pinocytosis or receptor-mediated endocytosis and which localized in the cytoplasm did not cause any measurable effets on T cell function (Sundstrom et al., 2004). Therefore, highly specific biological, biochemical and biophysical properties are required to develop drug-derivatized SPIONs that can detect lesions and that are capable of tissue- and cell-selective drug delivery. The detection systems must be non-invasive, and the agents allowing detection must be biocompatible and biodegradable. In addition, cell activation and the production of inflammatory molecules must be avoided. Polymeric coating of SPIONs has been used to prevent nanoparticle aggregation in biological media to achieve non-invasive detection system in enhanced magnetic imaging. Once directed toward the target cells, the functionalized SPIONs can be immobilized at a particular site using external magnetic fields, thus providing an additional degree of control over the drug delivery. In addition, varying the biochemical characteristics of the coating polymer may allow for selective intracellular or extracellular delivery of the drugs to the target cells.

In conclusion, the successful development of biocompatible functionalized SPIONs capable of intracellular uptake by cells depends on several factors including size, surface area-to-volume ratio, physicochemical and biochemical properties of the coating shell, and the cell type. When aminoPVA-SPIONs were taken up by brain-derived structures, no evidence of inflammatory reaction was observed and no massive and deep invasion of the brain were observed. Injection of aminoPVA-SPIONs in normal mice demonstrated biocompatibility in living animals. The observation using Endorem and Sinerem that vascular leakage associated with multiple sclerosis and its experimental models can be documented, suggests that under pathological circumstances access to the brain of SPIONs can be obtained. Alternatively, drugs could be released from their carrier following uptake by the brain vasculature and diffuse to brain parenchyma, since the brain is one of the most densely vascularized organ,

and it is assumed that each vessel is separated from its neighbor by around 40 μm, which means that every neural cell almost has its private vessel and that once a drug has traversed the blood brain barrier its brain distribution is immediate. Therefore these nanostructures represent useful tools for further development of nanostructures able of intracellular delivery of therapeutic agents to brain cells.

Aknowledgements

We want to thank Dr P Ricciardi-Castagnoli, Milano, for the gift of microglial cell lines, Ms P Fioroni, C Chappuis-Bernasconi, and A Ferrari for excellent technical assistance.

References

Alexiou C, Arnold W, Klein RJ, Parak FG, Hulin P, Bergemann C, Erhardt W, Wagenpfeil S, Lübbe AS (2000) Locoregional cancer treatment with magnetic drug targeting. *Cancer Res* **60**:6641-6648.

Borm PJ, Kreyling W (2004) Toxicological hazards of inhaled nanoparticles – potential implications for drug delivery. *J Nanosci Nanotech* **4**:521-531.

Brigger I, Dubernet C, Couvreur P (2002) Nanoparticles in cancer therapy and diagnosis. *Adv Drug Deliv Rev* **54**:631-651.

Chastellain M, Petri A, Hofmann H (2004) Particle size investigations on a multi-step synthesis of PVA coated superparamagnetic nanoparticles. *J Colloid Interface Sci* **278**:353-360.

Chellat F, Merhi Y, Moreau A, Yahia L (2005) Therapeutic potential of nanoparticulate systems for macrophage targeting. *Biomaterials* **26**:7260-7275.

Colvin VL (2003) The potential environmental impact of engineered nanomaterials. *Nat Biotech* **21**:1166-1170.

Corot C, Petry KG, Trivedi R, Saleh A, Jonkmanns C, Le Bas JF, Blezer E, Rausch M, Brochet B, Foster-Gareau P, Baleriaux D, Gaillard S, Dousset V (2004) Macrophage imaging in central nervous system and in carotid atherosclerotic plaque using ultrasmall

superparamagnetic iron oxide in magnetic resonance imaging. *Invest Radiol* **39**:619-625.

Daldrup-Link HE, Rudelius M, Piontek G, Metz S, Brauer R, Debus G, Corot C, Schlegel J, Link TM, Peschel C, Rummeny EJ, Oostendorp RA (2005) Migration of iron oxide-labeled human hematopoietic progenitor cells in a mouse model: in vivo monitoring with 1.5-T MR imaging equipment. *Radiology* **234**:197-205.

Hoehn M, Kustermann E, Blunk J, Wiedermann D, Trapp T, Wecker S, Focking M, Arnold H, Hescheler J, Fleischmann BK, Schwindt W, Buhrle C (2002) Monitoring of implanted stem cell migration in vivo: a highly resolved in vivo magnetic resonance imaging investigation of experimental stroke in rat. *Proc Natl Acad Sci USA* **99**:16267-16272.

Hoet PHM, Brüske-Hohlfeld I, Salata OV (2004) Nanoparticles- known and unknown health risks. *J Nanobiotech* **2**:12-27.

Honegger P, Tschudi-Monnet F (2000) Aggregating neural cell cultures, in *Protocols for neural cell culture* (Fedoroff S, Richardson A, eds) pp 199-218, Humana Press, Inc, New Jersey.

Juillerat-Jeanneret L, Aguzzi A, Wiestler OD, Darekar P, Janzer RC (1992) Dexamethasone regulates the activity of enzymatic markers of cerebral endothelial cell lines. *In Vitro Cell Dev Biol* **28A**:537-543.

Juillerat-Jeanneret L, Monnet-Tschudi F, Zürich MG, Lohm S, Duijvestijn AM, Honegger P (2003) Regulation of peptidase activity in a three-dimensional aggregate model of brain tumor vasculature. *Cell Tissue Res* **311**:53-59.

Kandimalla KK, Donovan MD (2005) Carrier mediated transport of chlorpheniramine and chlorcyclizine across bovine olfactory mucosa:implications on nose-to-brain transport. *J Pharm Sci* **94**:613-624.

Kircher MF, Mahmood U, King RS, Weissleder R, Josephson L (2003) A multimodal nanoparticle for preoperative magnetic resonance imaging and intraoperative optical brain tumor delineation. *Cancer Res* **63**:8122-8125.

Koch AM, Reynolds F, Merkle HP, Weissleder R, Josephson L (2005) Transport of surface-modified nanoparticles through cell monolayers. *ChemBioChem* **6**:337-345.

Kreuter J (2004) Influence of the surface properties on nanoparticles-mediated transport of drugs to the brain. *J Nanosci Nanotech* **4**:484-488.

Lockman PR, Oyewumi MO, Koziara JM, Roder KE, Mumper RJ, Allen DD (2003) Brain uptake of thiamine-coated nanoparticles. *J Control Rel* **93**:271-282.

Lockman PR, Koziara JM, Mumper RJ, Allen DD (2004) Nanoparticle surface charges alter blood-brain barrier integrity and permeability. *J Drug Target* **12**:635-641.

Lubbe AS, Bergemann C, Huhnt W, Fricke T, Riess H, Brock JW, Huhn D (1996) Preclinical experiences with magnetic drug targeting: tolerance, and efficacy. *Cancer Res* **56**:4694-4701.

Massart R, Dubois E, Cabuil V, Hasmonay E (1995) Preparation and properties of monodisperse magnetic fluids. *J Mag Mag Materials* **149**:1-5.

Muldoon LL, Pagel MA, Kroll RA, Roman-Goldstein S, Jones RS, Neuwelt EA (1999) A physiological barrier distal to the anatomic blood-brain barrier in a model of transvascular delivery. *Am J Neuroradiol* **20**:217-222.

Muller RH, Keck CM (2004) Drug delivery to the brain – realization by novel drug carriers. *J Nanosci Nanotech* **4**:471-483.

Murata JI, Betz Corradin S, Janzer RC, Juillerat-Jeanneret L (1994) Tumor cells suppress cytokine-induced nitric oxide (NO) production in cerebral endothelial cells. *Int J Cancer* **59**:699-705.

Murata JI, Ricciardi-Castagnoli P, Dessous L'Eglise Mange P, Martin F, Juillerat-Jeanneret L (1997) Microglial cells induce cytotoxic effects towards colon carcinoma cells :measurement of tumor cytotoxicity with a g-glutamyl transpeptidase assay. *Int J Cancer* **70**:169-174.

Neuwelt EA, Varallyay P, Bago AG, Muldoon LL, Nesbit G, Nixon R (2004) Imaging of iron oxide nanoparticles by MR and light microscopy in patients with malignant brain tumors. Neuropath. *Appl Neurobiol* **30**:456-471.

Obersdörster G, Sharp Z, Atudorei V, Elder A, Gelein R, Kreyling W, Cox C (2004) Translocation of inhaled ultrafine particles to the brain. Inhalation *Toxicol* **16**:437-445.

Perry VH, Andersson PB, Gordon S (1993) Macrophages and inflammation in the central nervous system. *TINS* **16**:268-273.

Petri-Fink A, Chastellain M, Juillerat-Jeanneret L, Ferrari A, Hofmann H (2005) Development of functionalized superparamagnetic iron oxide nanoparticles for interaction with human cancer cells. *Biomaterials* **26**:639-646.

Raynal I, Rrigent P, Peyramaure S, Najid A, Rebuzzi C, Corot C (2004) Macrophage endocytosis of superparamagnetic iron oxide nanoparticles:mechanisms and comparison of ferrumoxides and ferrumoxtran-10. *Invest Rad* **39**:56-63.

Risau W, Wolburg W (1990) Development of blood-brain barrier. *TINS* **13**:174-178.

Rudge S, Peterson C, Vessely C, Koda J, Stevens S, Catterall L (2001) Adsorption and desorption of chemotherapeutic drugs from a magnetically targeted carrier (MTC). *J Control Rel* **74**:335-340.

Ruehm SG, Corot C, Vogt P, Kolb S, Debatin JF (2001) Magnetic resonance imaging of atherosclerotic plaque with ultrasmall superparamagnetic particles of iron oxide in hyperlipidemic rabbits. *Circulation* **103**:415-422.

Savic R, Luo L, Eisenberg A, Maysinger D (2003) Micellar nanocontainers distribute to defined cytoplasmic organelles. *Science* **300**:615-618.

Sundstrom JB, Mao H, Santoianni R, Villinger F, Little DM, Huynh TT, Mayne AE, Hao E, Ansari AA (2004) Magnetic resonnance imaging of activated proliferating rhesus macaque T cells labeled with superparamagnetic monocristalline iron oxide nanoparticles. *J AIDS* **35**:9-21

Triverdi RA, U-King-Im JM, Graves MJ, Cross JJ, Horsley J, Goddard MJ, Skepper JN, Quartey G, Warburton E, Joubert I, Wang L, Kirkpatrick PJ, Brown J, Gillard JH (2004) In vivo detection of macrophages in human carotid atheroma. Temporal dependence of ultrasmall superparamagnetic particles of iron oxide-enhanced MRI. *Stroke* **35**:1631-1635.

van Ewijk GA, Vroege GJ, Philipse AP (1999) Convenient preparation methods for magnetic colloids. *J Mag Mag Materials* **201**:31-33.

Weissleder R, Cheng HC, Bogdanova A, Bogdanov A (1997) Magnetically-labeled cells can be detectected by MR imaging. *J Magn Reson Imaging* **7**:258-263.

Wilhelm C, Billotey C, Roger J, Pons JN, Bacri JC, Gazeau F (2003) Intracellular uptake of anionoic superparamagnetic nanoparticles as a function of their surface coating. *Biomaterials* **24**:1001-1011.

Zhang Y, Kohler N, Zhang M (2002) Surface modification of superparamagnetic magnetite nanoparticles and their intracellular uptake. *Biomaterials* **23**:1553-1561.

Footnotes

Financial support: This works was supported by grants from the Swiss National Scientific Research Foundation (grant No 3152A0-105705), the Swiss League and Research against Cancer (grant No KLS-01308-02-2003), Guerbet France, the EU project Magnanomed, and the Swiss Society for Multiple Sclerosis.

JPET Fast Forward. Published on April 11, 2006 as DOI: 10.1124/jpet.106.101915
This article has not been copyedited and formatted. The final version may differ from this version.

Legends for Figures

Figure 1: *Structures of the various SPIONs (A) and PVA (B) used in this study.*

Figure 2: *Uptake of Endorem by N11 microglial cells as a function of the amount of SPIONs added to cells.*

Murine N11 microglial cells were exposed to increasing concentrations of Endorem for 16 h. Then cell-bound iron was measured using the Prussian Blue reaction and means ± SD were calculated. Experiments were repeated twice in triplicate wells.

Figure 3*: *Uptake of functionalizedPVA-SPIONs by N11 microglial cells and EC219 endothelial cells as a function of the amount of SPIONs added to cells.

Murine N11 microglial (A) or rat EC219 endothelial cells (B) were exposed to increasing concentrations of functionalizedPVA-SPIONs for 2 h . Then cell-bound iron was measured using the Prussian Blue reaction and means ± SD were calculated. Experiments were repeated twice in triplicate wells.

Figure 4: *Uptake of aminoPVA-SPIONs by brain-derived endothelial and microglial cells*

EC219 (A) or N11 (B) cells were grown on histological slides in culture medium, then exposed to aminoPVA-SPIONs (5 µg iron/ml, final concentration) for up to 4 h. Cellular iron content was determined *in situ* using Prussian Blue reaction adapted for histological determination. Scale bar = 20 µm.

Figure 5: *Uptake of Cy3.5-aminoPVA-SPIONs by brain-derived microglial cells*

(A) AminoPVA-SPIONs were derivatized with Cy3.5, and characterized, ◆: size distribution; □ : dye/particles ratio.

(B and C). Cells were grown in culture medium in culture wells, then exposed to Cy3.5-SPIONs (4-83 μg iron/ml, final concentration) for 2 h or 4 h, either at 4°C or 37°C. Then following extensive washing, Cy3.5 fluorescence was measured in the intact cell layer (B), followed by cellular iron content determined using Prussian Blue reaction (C) in cell extracts.

Figure 6: *Confocal micrographs of N9 murine microglial cells exposed to Cy3.5-aminoPVA-SPIONs.*

N9 cells were incubated with Cy3.5-aminoPVA-SPIONs (20 μg iron/ml, final concentration) for time interval between 1 min to 20 h. There was no detectable signal after 1min and weak signal after 10 min (not shown). After 20 min, cell morphology was normal (Figure 5A, first panel) and membrane labeling by green fluorescent dye DAF (1 μM, 1 min, Figure 5A, last panel), but no Cy3.5 signal was detected (Figure 5A, middle panel). After 20 h, cells retained their morphology (Figure 5B, first panel), and displayed intense Cy3.5 signal (Figure 5B, middle panel). Superimposed images (Figure 5B, last panel) from green fluorescent dye DAF (1 μM, 1 min), DAPI (10 μM, 10 min) and Cy3.5 revealed cytosolic location of the SPIONs corroborating the data of cell-bound iron obtained after 0, 30 or 240 min with phase contrast microscopy (Figure 5C, arrows). Scale bar = 20 μm.

Figure 7: *Uptake of aminoPVA-SPIONs by rat brain-cell aggregates.*

A: Differentiating brain-cell aggregates after 1, 2, 3 or 4 weeks of culture and differentiation, were exposed for 3 days to aminoPVA-SPIONs, and culture was continued for 2 other days without aminoPVA-SPIONs. Iron was determined on histological slides by Prussian Blue reaction (blue staining, cell nuclei are red).

B: microglial cells activation was controlled by BS-1 lectin staining (dark brown staining).

JPET Fast Forward. Published on April 11, 2006 as DOI: 10.1124/jpet.106.101915
This article has not been copyedited and formatted. The final version may differ from this version.

Table 1 : *Physical characteristics (size, morphology, coating and surface properties) of the SPIONs and beads used.*

Particle	Diameter of the magnetic core [nm]	Hydrodynamic diameter [nm]	Morphology	Coating	Surface charge
Endorem*	**4-6**	**80 - 150**	**Bead****	**Dextran**	**neutral**
Sinerem*	**4-6**	**30**	**Single particle**	**Dextran**	**neutral**
PVA-SPIONs	**8-12**	**30**	**Single particle**	**PVA**	**neutral**
AminoPVA-SPIONs	**8-12**	**30**	**Single particle**	**AminoPVA**	**positive**
CarboxyPVA-SPIONs	**8-12**	**30**	**Single particle**	**CarboxyPVA**	**negative**
ThiolPVA-SPIONs	**8-12**	**30**	**Single particle**	**ThiolPVA**	**negative**

*** Values given by Guerbet**

**** Beads are particles with several nanosized iron oxide particles embedded in a matrix (in this case dextran)**

JPET Fast Forward. Published on April 11, 2006 as DOI: 10.1124/jpet.106.101915
This article has not been copyedited and formatted. The final version may differ from this version.

Table 2 : *Sinerem uptake by rodent brain-derived EC219 endothelial cells or murine N9 and N11 microglial cells.*

Rat brain-derived EC219 endothelial cells were exposed to Sinerem (0, 1.8 or 3.5 mM iron equivalents added at t=0) or murine N9 and N11 microglial cells were exposed to Sinerem (1.8 mM iron equivalents added at t=0) for 2, 6 or 24 h. Then cell-bound iron was measured using the Prussian Blue reaction and means ± SD were calculated. Experiments were repeated twice in triplicate wells.

	EC 219 cells			***N9 cells***	***N11 cells***
iron added	*0*	*1.8*	*3.5*	*1.8*	*1.8* *[mM]*
Time[h]	***cell-bound iron[μM]***				
2	53±9	59±6	59±5	59±9	110±11
6	51±9	51±8	51±6	48±8	144±16
24	61±8	59±9	59±6	nd	nd

nd: not done

JPET Fast Forward. Published on April 11, 2006 as DOI: 10.1124/jpet.106.101915
This article has not been copyedited and formatted. The final version may differ from this version.

Table 3 : *Co-culture of brain-derived EC219 endothelial cells and N9 (A) or N11 (B) microglial cells did not increase Sinerem uptake by cells.*

Cells were grown either alone or together for 24 h, then Sinerem (1.8 mM iron equivalents) was added at t=0 simultaneously (+) with LPS or without (-) LPS, and cell-bound iron was measured using the Prussian Blue reaction and means ± SD were calculated.

A)	***N9***		***EC219 + N9***	
	-	**+**	**-**	**+** ***LPS***
Time[h]	***cell-bound iron[μM]***			
8	34±6	34±9	53±9	53±6
24	48±8	48±6	59±10	59±11
35	48±8	48±7	48±8	54±8

B)	***N11***		***EC219 + N11***	
	-	**+**	**-**	**+** ***LPS***
Time[h]	***cell-bound iron[μM]***			
8	50±9	50±11	53±8	53±9
24	53±8	53±11	58±12	62±11
35	54±8	53±9	42±11	42±12

Table 4 : *Endorem uptake by rodent brain-derived EC219 endothelial cells or murine N11 microglial cells.*

Rat brain-derived EC219 endothelial cells were exposed to Endorem (0.4 mM iron equivalents added at t=0 simultaneously (+) with LPS or without (-) LPS) or murine N11 microglial cells were exposed to Endorem (1.0 mM iron equivalents added at t=0 simultaneously (+) with LPS or without (-) LPS) for 16 or 24 h. Then cell-bound iron was measured using the Prussian Blue reaction and means ± SD were calculated. Experiments were repeated twice in triplicate wells.

	EC 219		**N11**		
	-	**+**	**-**	**+**	***LPS***
Time [h]	***cell-bound iron [μM]***				
16	54±11	53±10	102±19	166±24	
24	62±15	54±12	122+19	214±32	

JPET Fast Forward. Published on April 11, 2006 as DOI: 10.1124/jpet.106.101915
This article has not been copyedited and formatted. The final version may differ from this version.

A

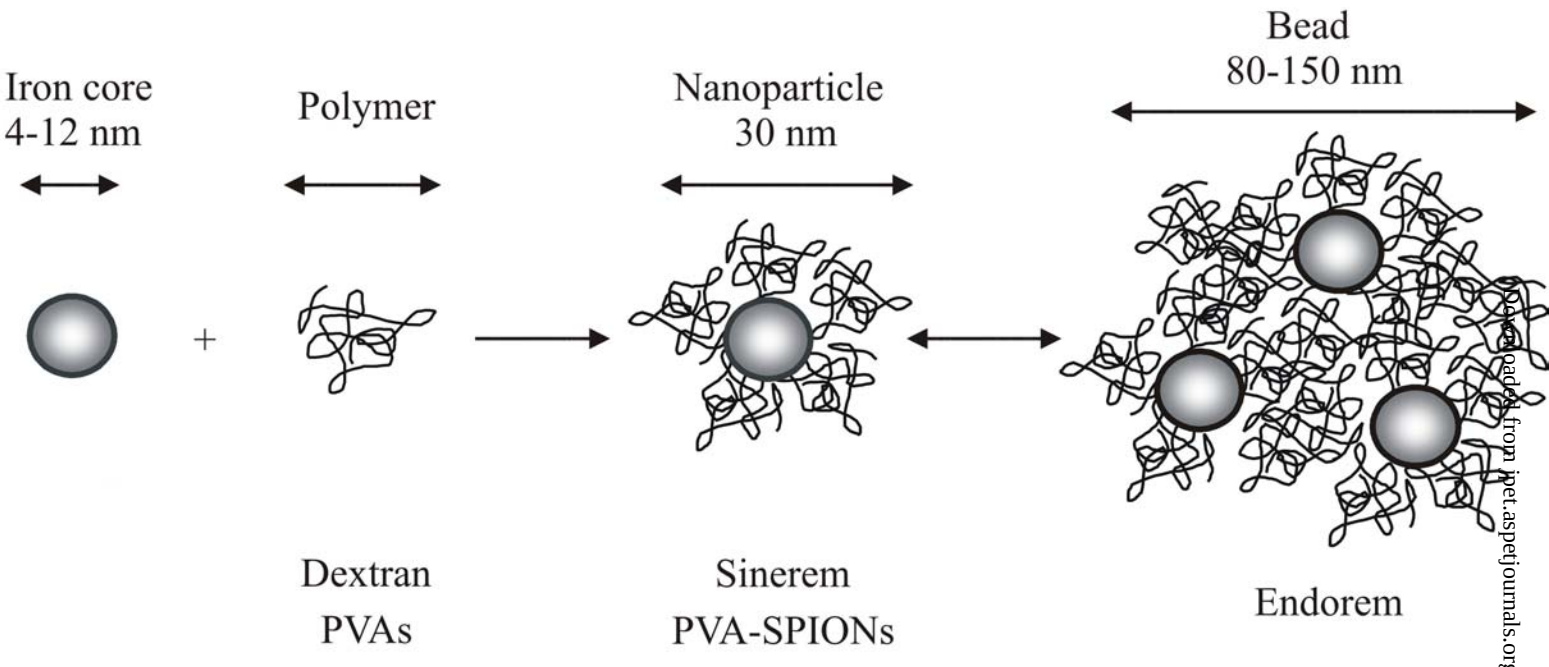

B

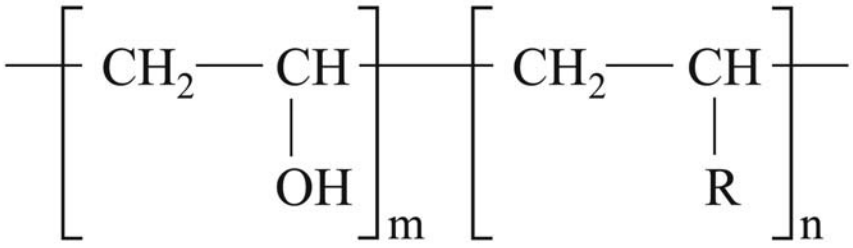

Polyvinyl alcohols (PVA):

PVA:	R=OH
aminoPVA :	R=NH_2
carboxyPVA :	R=COOH
thiolPVA :	R=SH

JPET Fast Forward. Published on April 11, 2006 as DOI: 10.1124/jpet.106.101915
This article has not been copyedited and formatted. The final version may differ from this version.

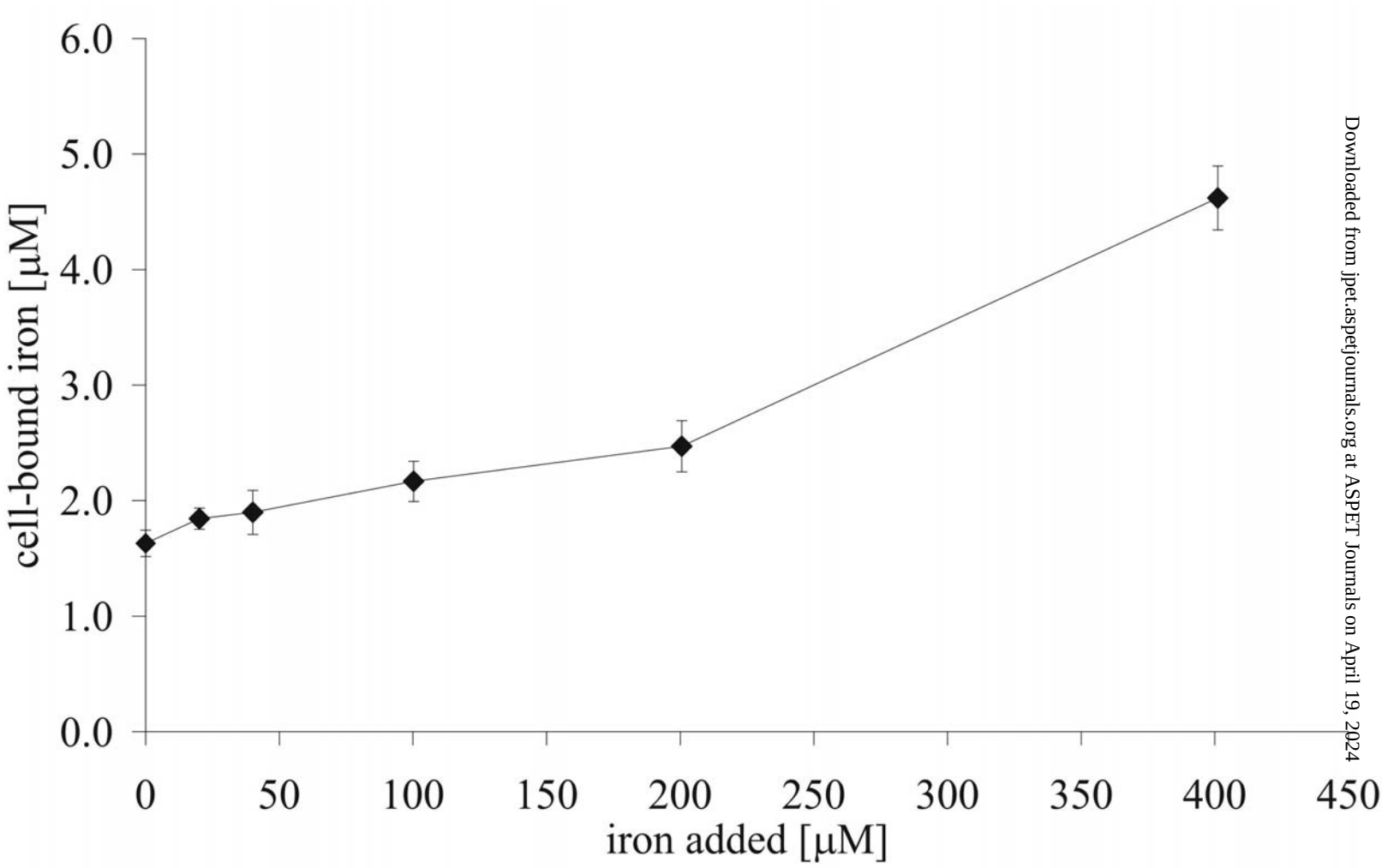

JPET Fast Forward. Published on April 11, 2006 as DOI: 10.1124/jpet.106.101915
This article has not been copyedited and formatted. The final version may differ from this version.

A

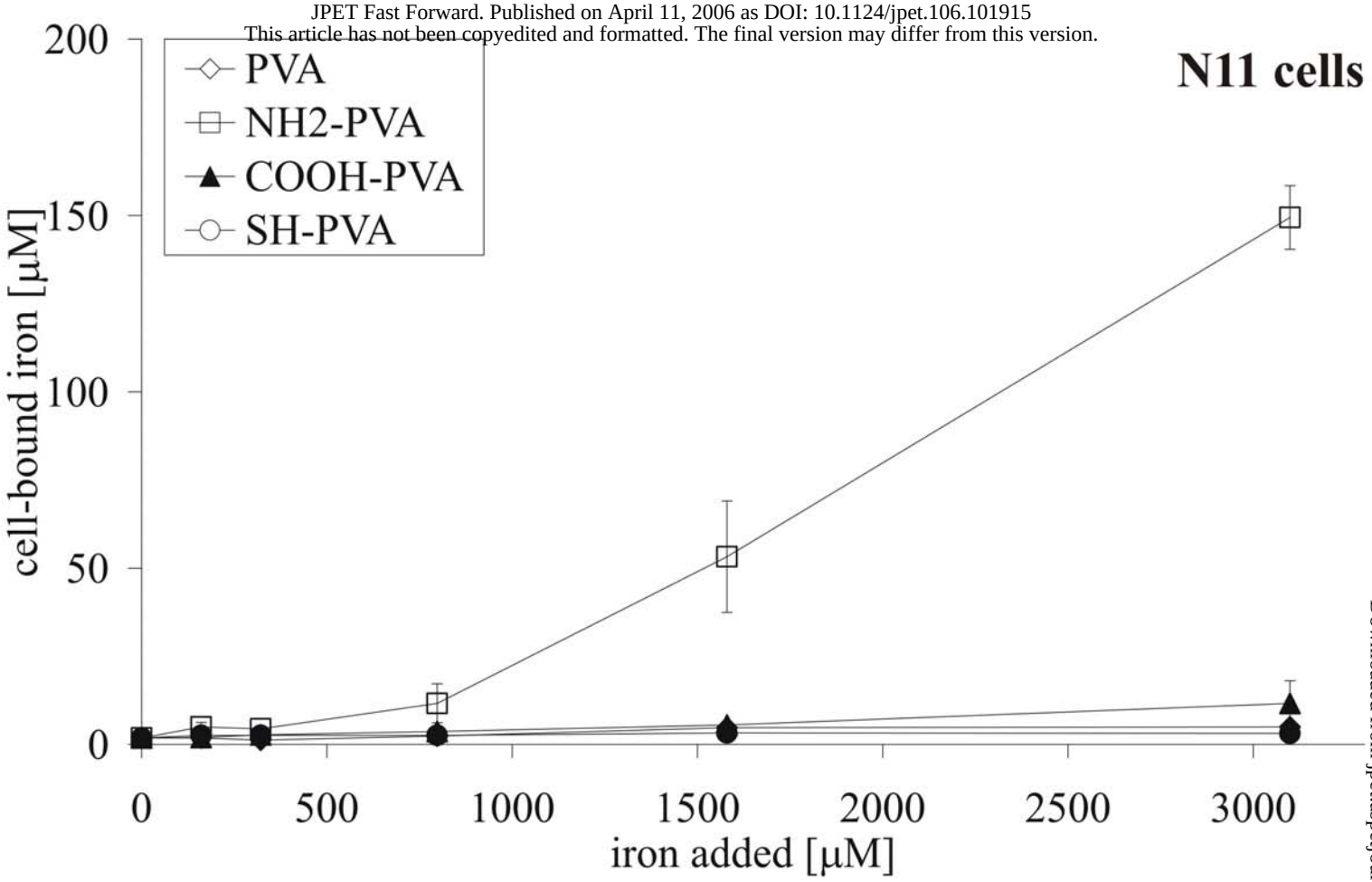

B

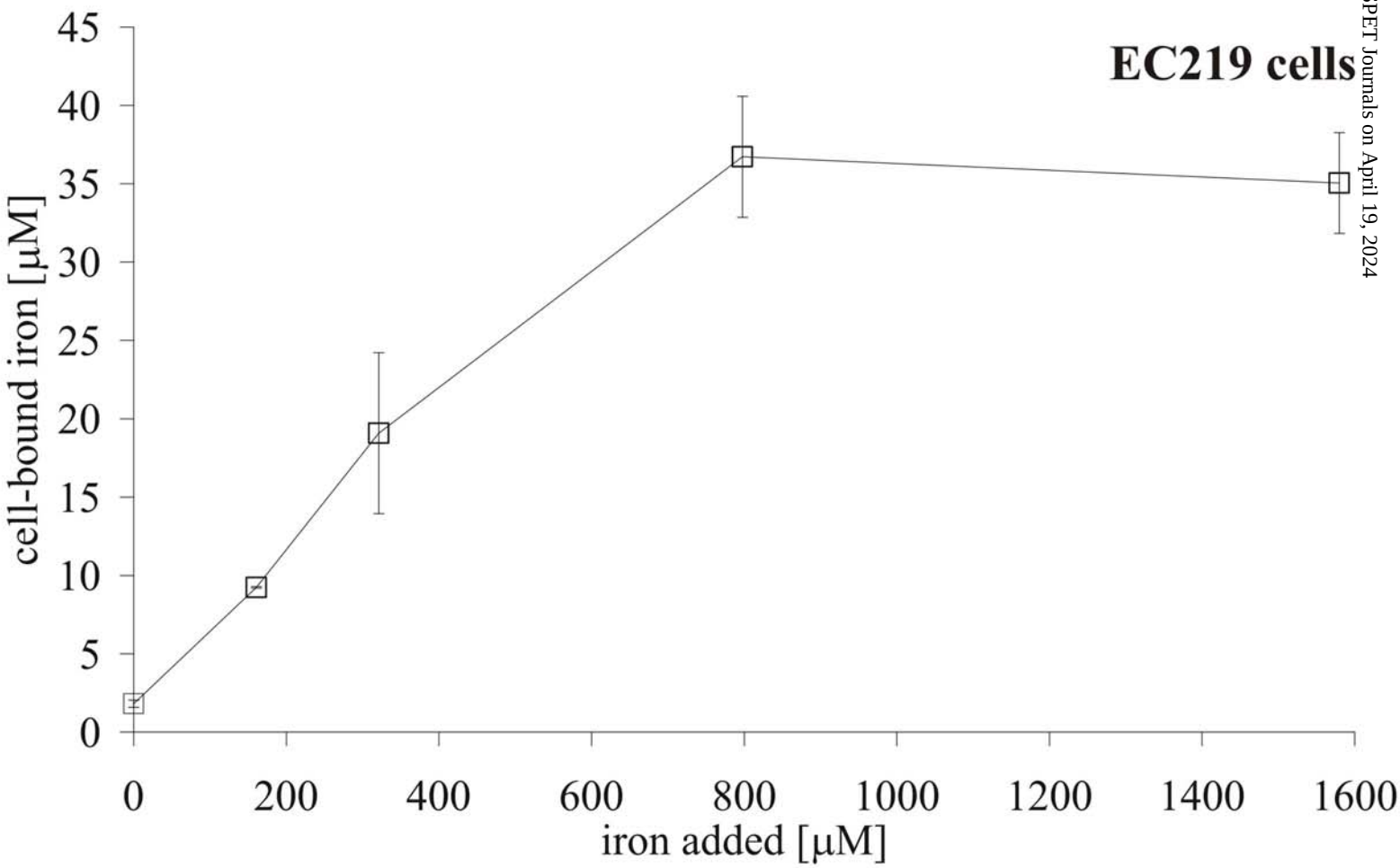

JPET Fast Forward. Published on April 11, 2006 as DOI: 10.1124/jpet.106.101915
This article has not been copyedited and formatted. The final version may differ from this version.

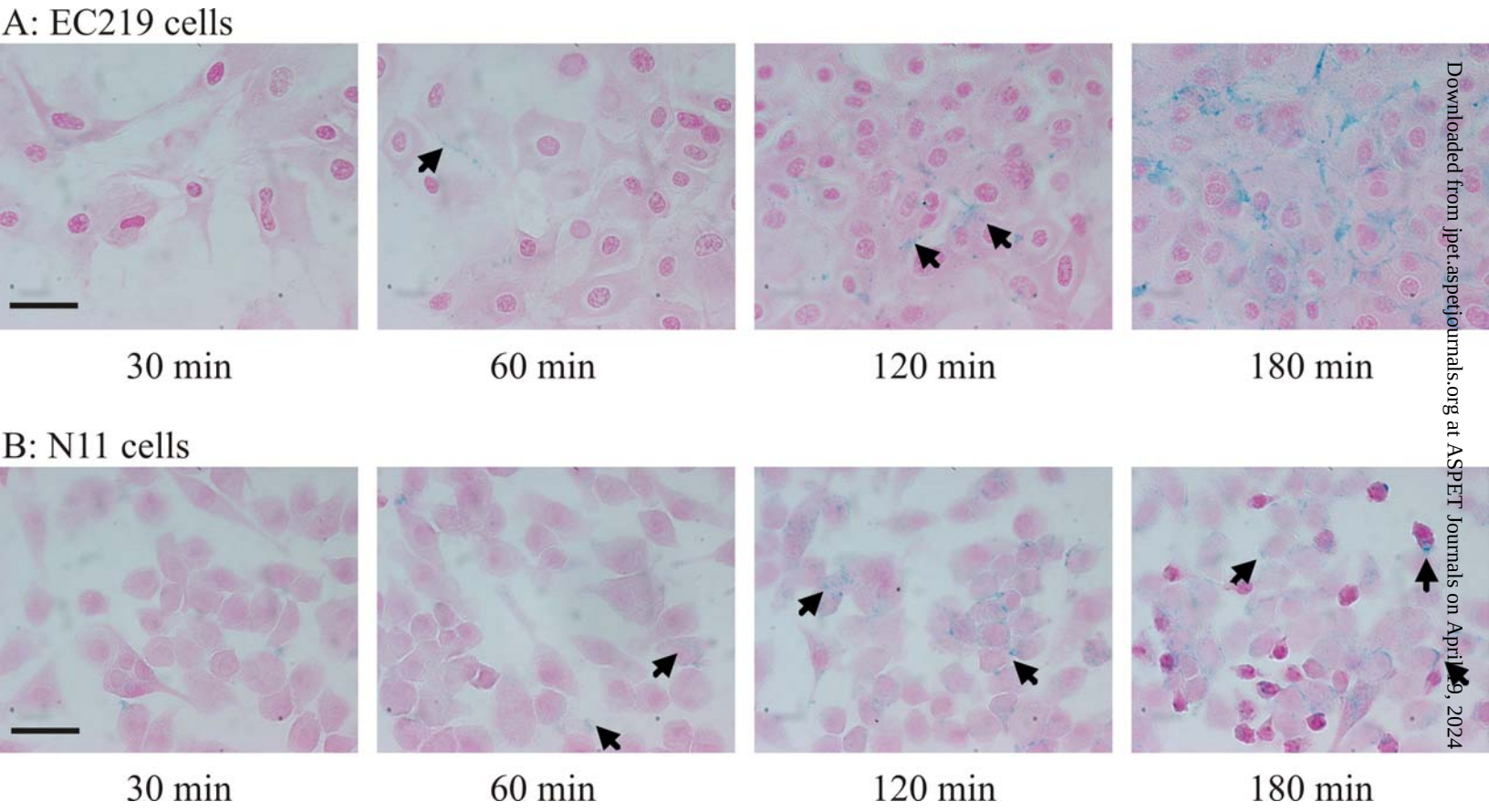

JPET Fast Forward. Published on April 11, 2006 as DOI: 10.1124/jpet.106.101915
This article has not been copyedited and formatted. The final version may differ from this version.

A

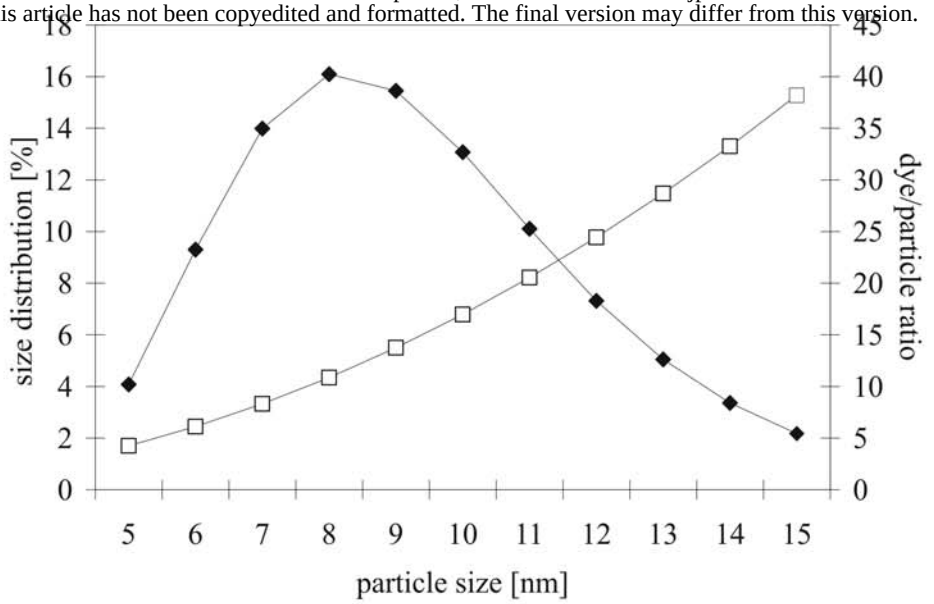

B

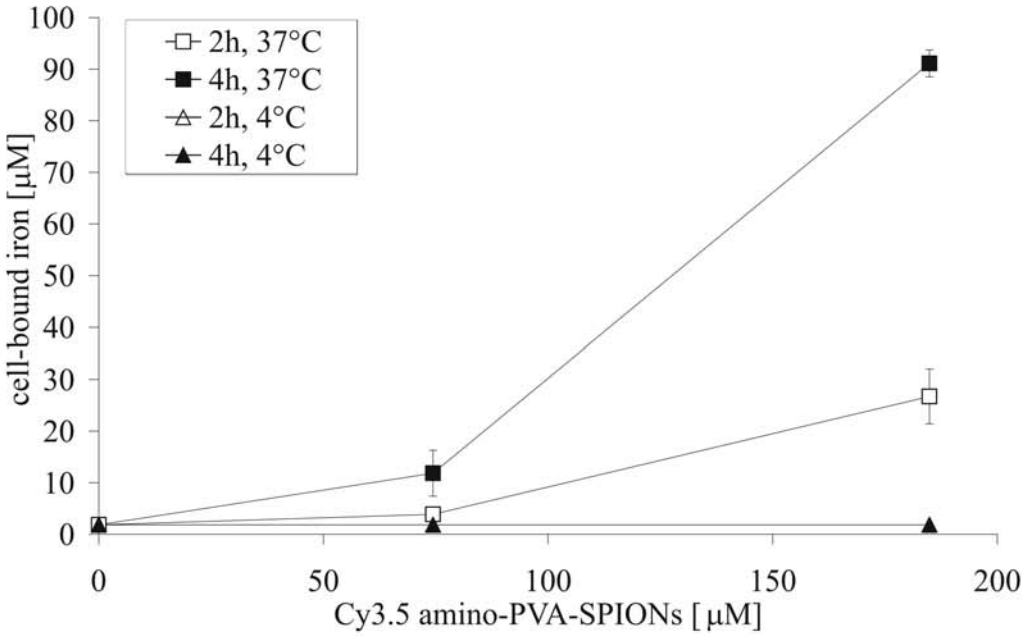

C

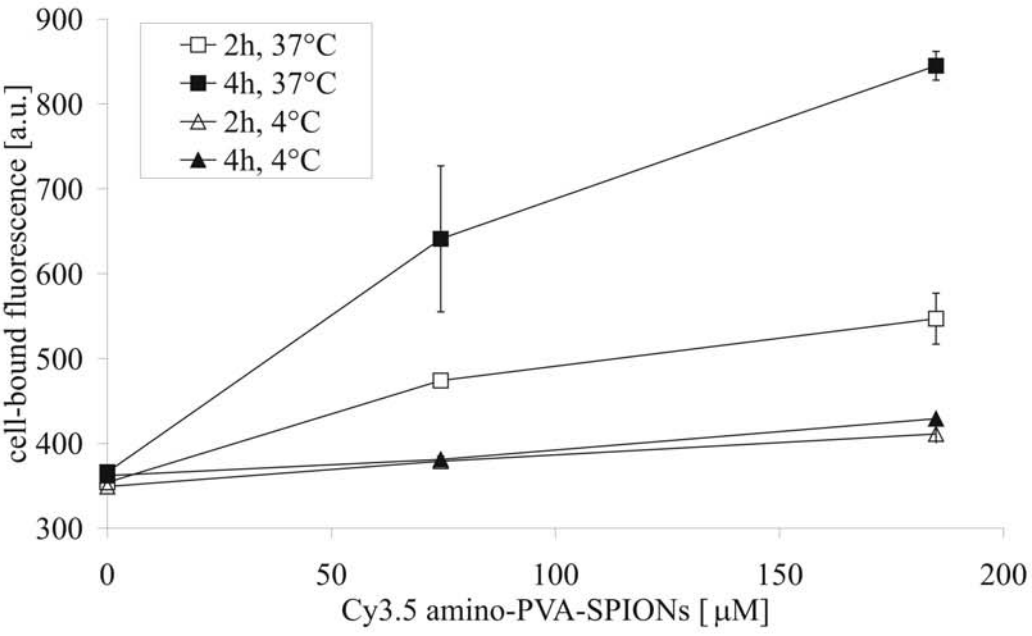

JPET Fast Forward. Published on April 11, 2006 as DOI: 10.1124/jpet.106.101915
This article has not been copyedited and formatted. The final version may differ from this version.

A: 20 min

phase contrast | Cy3.5 fluorescence | Cy3.5 and DAF fluorescence

B: 20 h

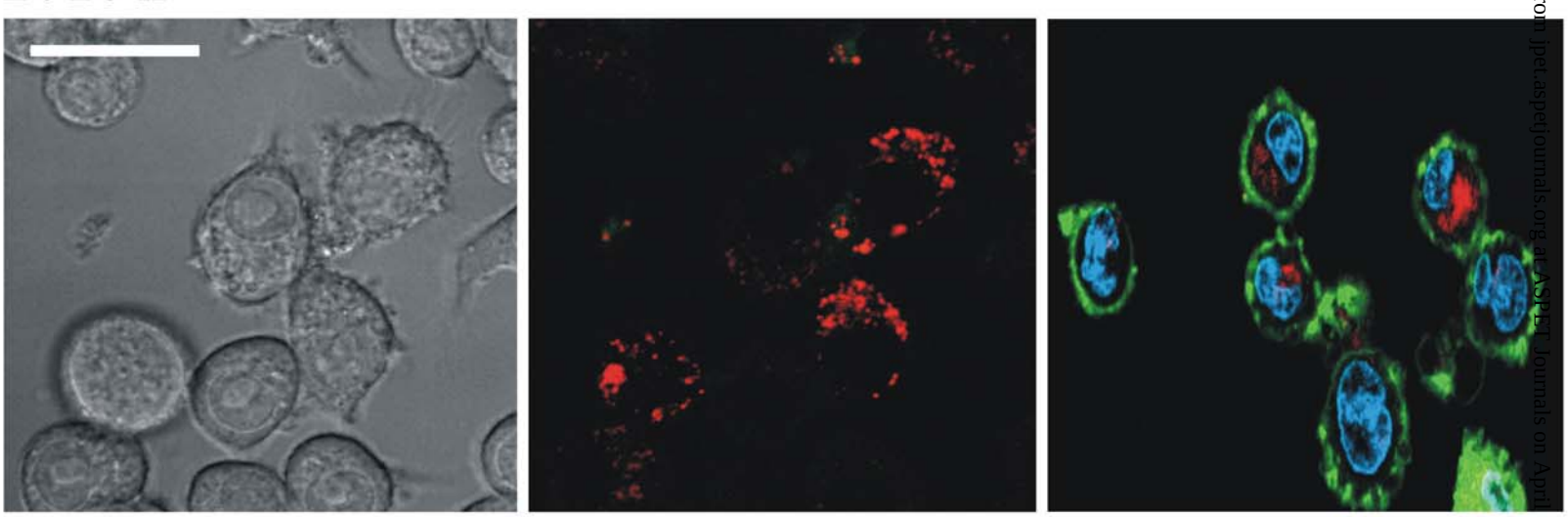

phase contrast | Cy3.5 fluorescence | Cy3.5, DAF, DAPI fluorescence

C: iron

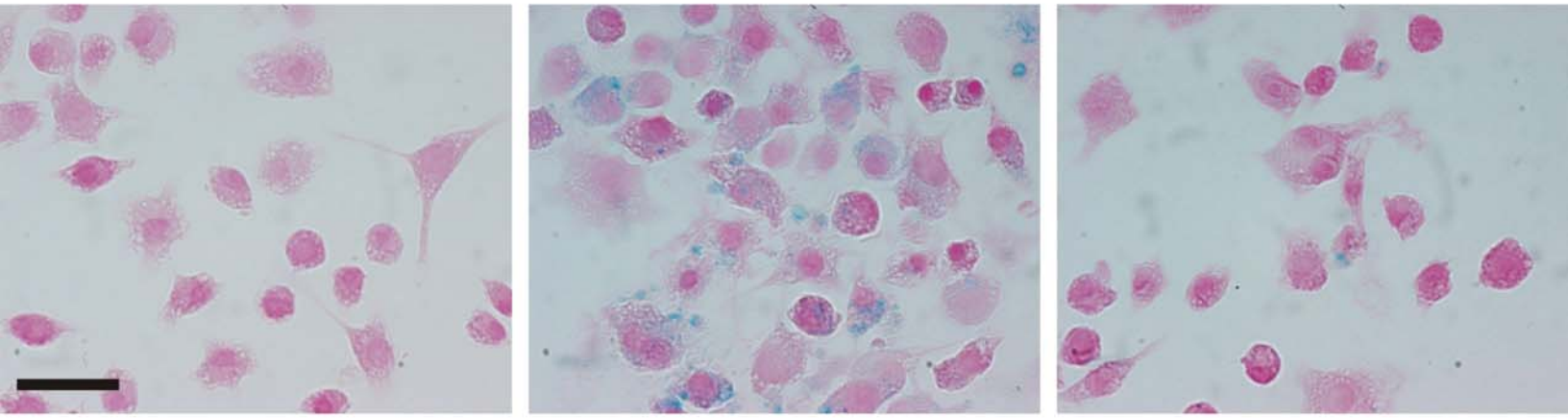

0 min | 30 min | 240 min

JPET Fast Forward. Published on April 11, 2006 as DOI: 10.1124/jpet.106.101915
This article has not been copyedited and formatted. The final version may differ from this version.

A

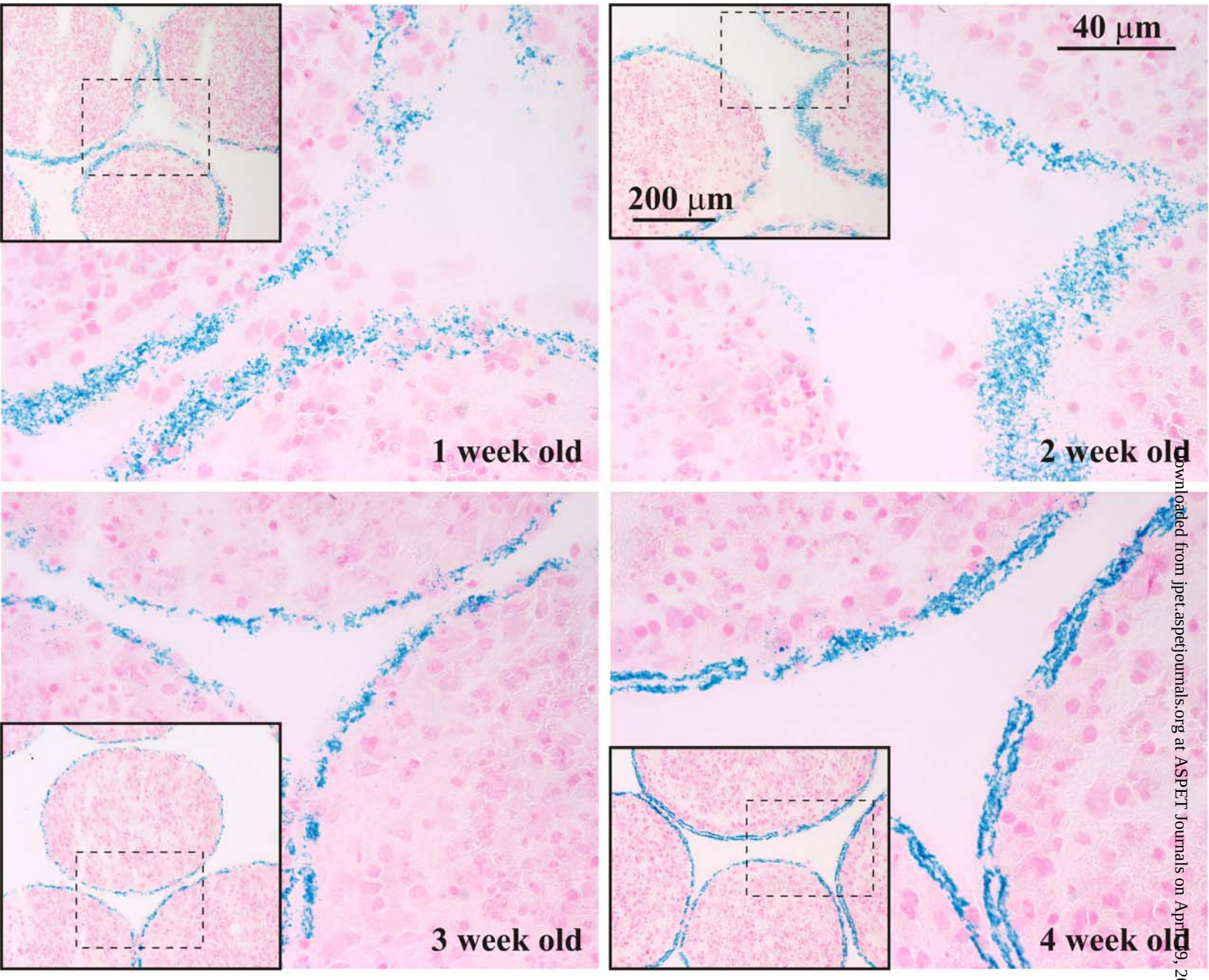

B